J. Membrane Biol. 158, 241–256 (1997)

The Journal of
Membrane
Biology

K^+-Sensitive Gating of the K^+ Outward Rectifier in *Vicia* Guard Cells

M.R. Blatt[1], **D. Gradmann**[2]

[1]Laboratory of Plant Physiology and Biophysics, University of London, Wye College, Wye, Kent TN25 5AH UK
[2]Pflanzenphysiologisches Institut, Universität Göttingen, Untere Karspüle 2, D-37073 Göttingen

Received: 27 November 1996/Revised: 4 March 1997

Abstract. The effect of extracellular cation concentration and membrane voltage on the current carried by outward-rectifying K^+ channels was examined in stomatal guard cells of *Vicia faba* L. Intact guard cells were impaled with double-barrelled microelectrodes and the K^+ current was monitored under voltage clamp in 0.1–30 mM K^+ and in equivalent concentrations of Rb^+, Cs^+ and Na^+. From a conditioning voltage of −200 mV, clamp steps to voltages between −150 and +50 mV in 0.1 mM K^+ activated current through outward-rectifying K^+ channels ($I_{K,out}$) at the plasma membrane in a voltage-dependent fashion. Increasing $[K^+]_o$ shifted the voltage-sensitivity of $I_{K,out}$ in parallel with the equilibrium potential for K^+ across the membrane. A similar effect of $[K^+]_o$ was evident in the kinetics of $I_{K,out}$ activation and deactivation, as well as the steady-state conductance-(g_{K^-}) voltage relations. Linear conductances, determined as a function of the conditioning voltage from instantaneous *I-V* curves, yielded voltages for half-maximal conductance near −130 mV in 0.1 mM K^+, −80 mV in 1.0 mM K^+, and −20 mV in 10 mM K^+. Similar data were obtained with Rb^+ and Cs^+, but not with Na^+, consistent with the relative efficacy of cation binding under equilibrium conditions ($K^+ \geqslant Rb^+ > Cs^+ > > Na^+$). Changing Ca^{2+} or Mg^{2+} concentrations outside between 0.1 and 10 mM was without effect on the voltage-dependence of g_K or on $I_{K,out}$ activation kinetics, although 10 mM $[Ca^{2+}]_o$ accelerated current deactivation at voltages negative of −75 mV. At any one voltage, increasing $[K^+]_o$ suppressed g_K completely, an action that showed significant cooperativity with a Hill coefficient of 2. The apparent affinity for K^+ was sensitive to voltage, varying from 0.5 to 20 mM with clamp voltages near −100 to 0 mV, respectively. These, and additional data indicate that extracellular K^+ acts as a ligand and alters the voltage-dependence of $I_{K,out}$ gating; the results implicate K^+-binding sites accessible from the external surface of the membrane, deep within the electrical field, but distinct from the channel pore; and they are consistent with a serial 4-state reaction-kinetic model for channel gating in which binding of two K^+ ions outside affects the distribution between closed states of the channel.

Key words: K^+ conductance — Voltage-dependent channel gating — K^+-dependent/stochastic gating model

Introduction

It is generally recognized that the outward-rectifying K^+ channels of guard cells provide the dominant pathway for K^+ efflux during stomatal closure (Blatt, 1991; Schroeder, 1992; Blatt & Thiel, 1993). Activation of these K^+ channels is evident on positive-going steps of membrane voltage (*V*) both in intact guard cells and in their protoplasts (Blatt & Thiel, 1993). It facilitates closure of the stomatal pore which is realized through a net efflux of osmotically active solutes from the guard cells — notably as a flux of K^+ from vacuole and cytoplasm across the plasma membrane — and the consequent decline in guard cell turgor. Ensemble current through these outward-rectifying K^+ channels ($I_{K,out}$) is augmented by the water-stress hormone abscisic acid (ABA) which promotes stomatal closure (Hetherington & Quatrano, 1991; MacRobbie, 1992; Blatt & Thiel, 1993), and some detail of the associated intracellular signal cascades is now understood (MacRobbie, 1991; Assmann, 1993; Blatt & Armstrong, 1993; Blatt & Thiel, 1993; Giraudat, 1995; Armstrong et al., 1995).

By contrast, little is known of the gating of $I_{K,out}$ and its relation to the ionic environment, although these intrinsic controls are crucial to channel function in vivo.

Correspondence to: M.R. Blatt

The channels do exhibit a moderate to high selectivity for K^+ over other alkali metal cations (Schroeder, Raschke & Neher, 1987; Hosoi, Iino & Shimizaki, 1988), although Na^+ can enter the K^+ channel from the cytoplasmic side before becoming lodged and blocking the channel pore. Block by intracellular Na^+ exhibits a strong voltage sensitivity, suggesting that the channel functions as a multi-ion pore and that block normally occurs with additional ions present in the channel (Thiel & Blatt, 1991).

Most striking are indications that the voltage-dependence of $I_{K,out}$ gating is sensitive to the concentration of extracellular K^+ and shifts in parallel with the K^+ equilibrium potential (E_K) in intact guard cells (Blatt, 1988; Blatt, 1991). The time-averaged steady-state current-voltage (*I-V*) relations for $I_{K,out}$ appear to be influenced by K^+ availability at the membrane exterior, whereas physiological charge flux through the channels depends on K^+ entering from the cytoplasmic side of the membrane. Furthermore, the corresponding single-channel conductance of the K^+ channels in these cells is largely unaffected by extracellular K^+ [(Schroeder et al., 1987) compare also (Hosoi et al., 1988; Ilan, Schwartz & Moran, 1994)]. Thus, an additional action of $[K^+]_o$ on the K^+ channels has been mooted, complementary to the voltage dependence for gating and distinct from ion permeation itself (Blatt, 1988; Blatt, 1991). Nonetheless, present models for gating of these K^+ channels (Schroeder, 1989; Van Duijn, 1993; Fairley-Grenot & Assmann, 1993; Ilan et al., 1994) do not account for the effect of $[K^+]_o$.

To gain a further understanding of the connection between K^+ and channel gating, we have explored effects of cations on the dynamic and steady-state characteristics of $I_{K,out}$. Here we report that $[K^+]_o$ affects $I_{K,out}$ activation and deactivation, without altering its apparent gating charge or maximum conductance, and with the net result that $[K^+]_o$ and membrane voltage act cooperatively to suppress the ensemble channel conductance, $g_{K,out}$. The results are described by a stochastic model for channel gating in which the $[K^+]_o$-binding is kinetically removed from the immediate transitions between the open state and the adjacent closed state of the channel. These, and additional results offer strong support for an action of extracellular K^+ on the K^+ channels in controlling $I_{K,out}$ in vivo.

Materials and Methods

Plant Culture and Experimental Protocol

Vicia faba L., cv. (Bunyan) Bunyard Exhibition was grown on vermiculite with Hoagland's Salts medium and epidermal strips were prepared as described previously (Blatt, 1992). Measurements were carried out in rapidly flowing solutions (10 ml/min ⁻20 chamber volumes/min). The standard perfusion medium was prepared with 5 mM 2-(N-morpholino)propanesulfonic acid (MES, pK_a = 6.1) or 4-(2-hydroxyethyl)-1-piperazine-ethanesulfonic acid (HEPES, pK_a = 7.4) and the buffers were titrated to their pK_as with $Ca(OH)_2$ (final $[Ca^{2+}]^-$ 1 mM). KCl, CsCl, RbCl and NaCl were included as required. Ambient temperatures were 20–22°C.

Microelectrodes

Recordings were obtained using double-barrelled microelectrodes coated with paraffin to reduce electrode capacitance (Blatt, 1992; Blatt & Armstrong, 1993). Current-passing and voltage-recording barrels were filled with 200 mM K^+-acetate, pH 7.5, to minimize salt leakage and salt-loading artifacts associated with the Cl^- anion (Blatt & Armstrong, 1993) without imposing a significant acid or alkaline load. Connection to the amplifier headstage was via a 1 M KCl|Ag-AgCl halfcell, and a matching halfcell and 1 M KCl-agar bridge served as the reference (bath) electrode.

Electrical

Mechanical, electrical and software design have been described in detail (Blatt, 1987*b*). Current-voltage (*I-V*) relations were determined by the two-electrode method with the voltage clamp under microprocessor control using a WyeScience μP amplifier and μLAB analog/digital interface and software (WyeScience, Wye, Kent). Steady-state *I-V* relations were recorded by clamping cells to a bipolar staircase of command voltages, alternating positive and negative from the free-running membrane potential, and currents and voltages were recorded during the final 10 msec of each pulse (Blatt, 1992; Blatt, 1987).

For kinetic characteristics, current and voltage were sampled continuously at 1, 2 or 10 kHz while the clamped potential was driven through cycles of 1–4, programmable pulse steps. In all cases the holding potential was set to *V* at the start of the clamp cycle and the current signal was filtered at 1 kHz. The sampling rate for most of the data shown was 2 kHz, although recordings at 10 kHz gave similar results. No attempt was made to compensate for the series resistance (R_S) to ground (Hodgkin, Huxley & Katz, 1952). Estimates for R_S indicated that it was unlikely to pose a serious problem in measurements of clamp potential (Blatt, 1988*b*).

Numerical Analysis and Kinetic Modelling

Data analysis was carried out by nonlinear, least-squares (Marquardt, 1963) and, where appropriate, results are reported as the mean ± SE of (n) observations.

For quantitative analysis of K^+ channel gating, the current traces and steady-stage g_K-*V* relationships obtained over a range of voltages and $[K^+]_o$ were jointly fitted by a Levenberg-Marquardt algorithm and least-squares minimisation (Press et al., 1986) to a serial (pseudo-) 3-state reaction scheme

$$C_3 \underset{k_{32}}{\overset{k_{23}}{\rightleftharpoons}} C_2 \underset{k_{21}}{\overset{k_{12}}{\rightleftharpoons}} O_1 \qquad [1]$$

with two closed states (C_3, C_2) and a terminal open state (O_1) defining the conductive conformation of the channel and k_{12}, k_{21}, k_{23} and k_{32} describing the reaction constants between states. The dynamic properties of this model are defined by the set of differential equations (Bertl, Kleiber & Gradmann, 1988)

$$-p_1\lambda = \frac{dp_1}{dt} = -k_{12}p_1 + k_{21}p_2 \quad [2a]$$

$$-p_2\lambda = \frac{dp_2}{dt} = k_{12}p_1 + k_{32}p_3 - (k_{21} + k_{23})p_2 \quad [2b]$$

$$-p_3\lambda = \frac{dp_3}{dt} = -k_{32}p_3 + k_{23}p_2 \quad [2c]$$

where p_1, p_2 and p_3 are the probabilities of residing in states O_1, C_2 and C_3, respectively, at the given voltage and λ denotes the eigenvalues of the equation ($\lambda = 1/\tau$, where τ is the corresponding relaxation time constant). Voltage dependence was introduced by assigning a voltage-sensitivity coefficient δ_{ij} to each reaction k_{ij} so that

$$k_{32} = k^o_{32}e^{\delta_{32}u},\ k_{23} = k^o_{23}e^{\delta_{23}u},\ k_{21} = k^o_{21}e^{\delta_{21}u},\ k_{12} = k^o_{12}e^{\delta_{12}u} \quad [3a–d]$$

Here $u = FV/RT$, where V is the membrane voltage and F, R and T have their usual meanings. The exponential terms thus correspond to a series of asymmetric Eyring barriers ($\delta_{ij} \neq \delta_{ji}$). The dependence on $[K^+]_o$ was assigned to one or more reaction steps as a coefficient of the reaction constant. Thus, for K^+ binding in the $C_2 \rightharpoonup C_3$ transition, $k_{23} = [K^+]_o k_{23}{}^o e^{\delta_{23}u}$ where $k_{23} = k^o_{23}$ when $V = 0$ mV and $[K^+]_o = 1$M.

At any given time t, the macroscopic current, $I(t)$, comprises a steady-state component I_s and a dynamic component comprising the sum of two exponential factors

$$I(t) = I_s + I_1e^{-\lambda_1 t} + I_2e^{-\lambda_2 t} \quad [4]$$

The steady-state current at each voltage is defined by the product of the ensemble open channel conductance g_o, the electrical driving force V-E_K, and the steady-state probability that the channel resides in state O_1

$$I_s = g_o(V - E_K)p_{1s} \quad [5]$$

where the steady-state open probability

$$p_{1s} = \frac{k_{32}k_{21}}{b} \quad [6a]$$

as derived from Eq. 2a for $dp_1/dt = 0$, and where

$$b = k_{32}k_{21} + k_{32}k_{12} + k_{12}k_{23} \quad [6b]$$

For the situation in which $[K^+]_o$-sensitivity is assigned to the $C_3 \leftrightharpoons C_2$ transition, Eq. 6a may be rewritten as

$$1/p_{1s} = 1 + K_1(1 + K_2) \quad [7a]$$

with

$$K_1 = k_{12}/k_{21} = (k^o_{12}/k^o_{21})e^{(\delta_{12}-\delta_{21})u}, \quad [7b]$$

$$K_2 = k_{23}/k_{32} = (k^o_{23}/k^o_{32})[K^+]_o^{m_{23}-m_{32}}\, e^{(\delta_{23}-\delta_{32})u}, \quad [7c]$$

and the mass action coefficients m_{32} and m_{23} representing the apparent $[K^+]_o$-sensitivity of the forward and reverse transitions.

The two relaxation constants in Eq. 4 are given by

$$\lambda_{1,2} = \frac{a}{2} \pm \frac{(a^2 - 4b)^{1/2}}{2} \quad [8a,b]$$

where $a = k_{32} + k_{23} + k_{12} + k_{21}$ and b is defined in Eq. 6b.

The current amplitudes I_1 and I_2 are defined by Δp_1 and Δp_2, the change in steady-state probabilities p_1 and p_2 on a voltage step, and give a time course for the current at any time t after the step in voltage according to Eq. 4 (Bertl et al., 1988) with

$$I_1 = \frac{\Delta p_1(k_{12} - \lambda_2) - \Delta p_2 k_{21}}{\lambda_1 - \lambda_2} g_o(V - E_K) \quad [9a]$$

and

$$I_1 = \frac{\Delta p_1(k_{12} - \lambda_1) - \Delta p_2 k_{21}}{\lambda_2 - \lambda_1} g_o(V - E_K) \quad [9b]$$

Current traces for analysis were selected from measurements with a common starting (holding) voltage either near the negative voltage extreme (typically −200 mV for activation kinetics) or at positive voltages (+20 or +50 mV for deactivation kinetics), and were corrected for background conductance determined from instantaneous currents [*see* Fig. 2; also Blatt, 1992]. These data were fitted to Eq. 4. Steady-state g_K-V relations (*see* Fig. 3) were fitted using Eq. 5. Analyses were carried out on data sets obtained from a single cell in each case, and the subsets of points — current traces and conductances — were fitted jointly with differences in reaction constants defined explicitly by the experimental variables V and $[K^+]_o$. Additionally, the residuals were adjusted to give equal weighting between data points within traces and between curves within data sets. Numerical values for each of the joint parameters k_{12}, k_{21}, k_{23}, k_{32}, δ_{12}, δ_{21}, δ_{23}, δ_{32}, and g_o were sought by sequential adjustment from starting values and analyses were repeated after initialising with different starting values to ensure that fittings converged on the same solution in every case. Because of the time during experiments required to gather these data (typically 30–40 min), the conductance maximum $g_{K,\max}$ was frequently observed to drift by as much as ±5–8%. In some analyses, therefore, g_o was allowed to vary by 5% between different $[K^+]_o$ data subsets. The ''hidden'' reaction constants k_{23}, k_{32}, k_{34}, k_{43}, and voltage sensitivity coefficients δ_{23}, δ_{32}, δ_{34} and δ_{43} of the extended reaction scheme [14] were determined numerically from the experimental variables and fitted values of the pseudo-3-state reaction constants k_{23} and k_{32} using Eq. 15.

Chemicals and Solutions

The pH buffers and salts were from Sigma Chemical (St. Louis, MO). Otherwise, all chemicals were Analytical Grade from BDH Ltd. (Poole, Dorset, UK).

Results

Steady-state Voltage and Current Characteristics

We took advantage of seasonal variations in H^+-ATPase activity (Blatt, 1990; Thiel, MacRobbie & Blatt, 1992; Blatt & Armstrong, 1993), and the sensitivity of the guard cell K^+ inward-rectifier to alkaline pH_o (Blatt & Armstrong, 1993; Blatt, 1992), to reduce the background of these currents. Comparing Figs. 1 and 2 shows that the electrical characteristics of the guard cells were dominated by $I_{K,\text{out}}$ under these conditions. Similar results were obtained in the other 48 cells exposed to concentrations ranging from 0.1 to 30 mM K^+ outside. For the data in Fig. 1, raising $[K^+]_o$ resulted in reversible

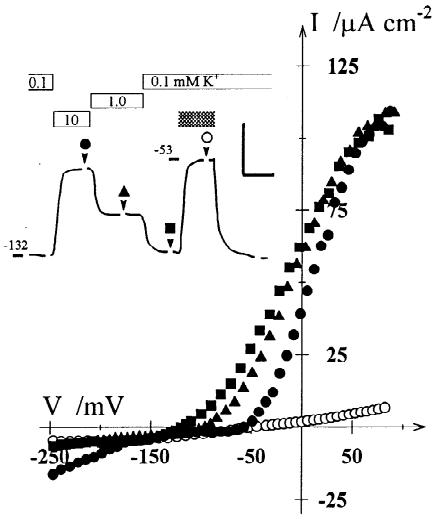

Fig. 1. A dominant outward current in the steady-state current-voltage (*I-V*) relations of *Vicia* stomatal guard cells. Raw currents recorded from one guard cell in 5 mM Ca^{2+}-HEPES, pH 7.4, with 0.1, 1.0 and 10 mM KCl as indicated (*inset*). Cell parameters: surface area, 1.6×10^{-5} cm^2; volume, 3.5 pl; aperture, 8.6 μm. Data gathered using a bipolar staircase protocol (*see* Materials and Methods) in 0.1 (■), 1.0 (▲), 10 mM KCl (●), and in 0.1 mM KCl with 10 mM TEA-Cl (○) to block the K^+ channels. Symbols cross-referenced to the voltage trace (*inset*). *Inset:* Free-running membrane voltage (in mV) with periods of exposures to KCl (open bars) and TEA-Cl (stippled bar) indicated above. Symbols mark times of voltage clamp scans (masked from trace) and cross-reference to the *I-V* curves. Scale: horizontal, 2 min; vertical, 50 mV.

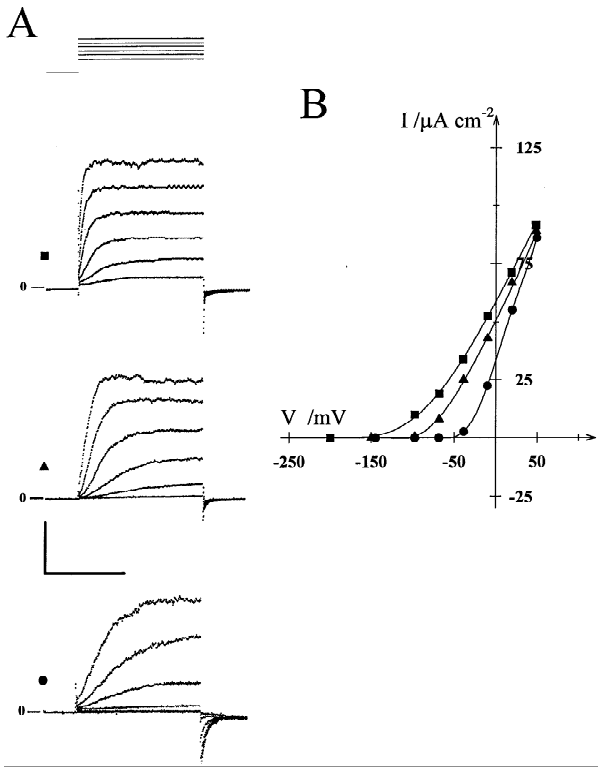

Fig. 2. The $[K^+]_o$- and voltage-dependence of the outward-rectifying K^+ channel current dominates the steady-state current-voltage (*I-V*) relations of *Vicia* stomatal guard cells. Data gathered concurrently with the raw *I-V* curves of Fig. 1 (symbols cross-referenced to Fig. 1), with the cell bathed in 0.1 (■), 1.0 (▲), 10 mM KCl (●). (*A*) Currents recorded at holding voltage of −150 mV (0.1 and 1 mM KCl) or −200 mV (10 mM KCl), on stepping to test voltages between −100 and +50 mV, and then on returning to the holding voltage. Scale: horizontal, 1 s; vertical, 50 μA cm^{-2} or 300 mV. (*B*) Ensemble steady-state K^+ channel *I-V* relations determined from the current traces in (*A*) after subtracting the background currents recorded 4 msec into each test voltage step. Background currents were determined separately as the ''instantaneous'' currents recorded 4 msec after positive-going voltage steps from −250 mV. [In some experiments with >3 mM $[K^+]_o$ these records were checked also with clamp steps from −150 mV to avoid possible distortion from $I_{K,in}$.]

positive changes in free-running voltage (Fig. 1, *inset*) from its resting value of −132 mV in 0.1 mM K^+ to −53 mV with 10 mM K^+ in the bath.

Clamping the membrane from a conditioning voltage negative of E_K to values between −100 and +50 mV yielded the characteristic time- and voltage-dependent activation of $I_{K,out}$ and its subsequent deactivation on returning the membrane to the conditioning voltage (Fig. 2*A;* see also Blatt & Armstrong (1993)). Raising $[K^+]_o$ had two effects on $I_{K,out}$: (i) it shifted the steady-state *I-V* curve along the voltage axis to more positive voltages, and (ii) it slowed $I_{K,out}$ activation upon positive voltage steps. The effect on the steady-state current is apparent in the raw, whole-membrane *I-V* curves (Fig. 1) and, for $I_{K,out}$, is evident in Fig. 2*B* after subtraction of background (''instantaneous'') currents [determined with clamp steps from −250 mV; see also Blatt (1992)] from the steady-state currents recorded at the end of each voltage step in Fig. 2*A.*

Extracellular K^+ Displaces the Steady-state Conductance of $I_{K,out}$

The data in Figs. 1 and 2 indicate a $[K^+]_o$ sensitivity to the voltage-dependence for gating of $I_{K,out}$. Nonetheless, quantifying any dependence of gating on $[K^+]_o$ must inevitably be complicated by the inherent asymmetry of the $[K^+]$ gradient across the membrane. For the ensemble channel current in this case

$$I_K = N\gamma_K p_o(V - E_K) \quad [10]$$

where N is the number of channels, γ_K their conductance in the open state, p_o the steady-state open probability (proportional to the relative conductance, $g_K/g_{K,max}$) and E_K the equilibrium potential. Nonlinearities may arise in both γ_K and in p_o. To distinguish bona fide differences in p_o from nonlinearities in γ_K, the voltage sensitivity of γ_K can be examined by plotting the instantaneous cur-

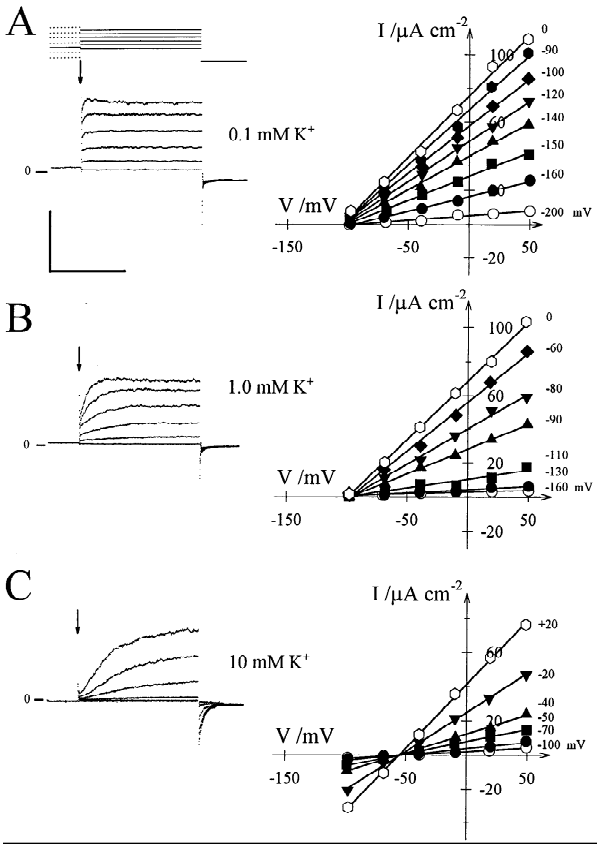

Fig. 3. Instantaneous K^+ channel current varies with $[K^+]_o$ and the conditioning voltage. Data from one guard cell recorded in 5 mM Ca^{2+}-HEPES, pH 7.4, with 0.1 (*A*), 1.0 (*B*) and 10 mM KCl (*C*) as indicated. Cell parameters: surface area, 1.9×10^{-5} cm^2; volume, 4.3 pl; aperture, 9.3 μm. Conductance analysis was carried out with test voltage steps to a common set of voltages from −100 to +50 mV, and the conditioning voltage was varied between each set of measurements (dashed lines at *top left* and voltages in mV on *far right*). Tailing voltages, −200 mV. *I-V* relations (*right*) taken from currents recorded 4 msec into test voltage steps (*arrows*, *left*). For the current traces shown (*left*), the conditioning voltage was −90 mV in each case. Scale (*left*): horizontal, 1 sec; vertical, 100 μA cm^{-2} or 500 mV.

rents recorded after voltage steps from conditioning voltages where the channel has an appreciable open probability and before p_o adjusts significantly toward the new steady-state.

Figure 3 illustrates three sets of measurements at concentrations 0.1, 1.0 and 10 mM $[K^+]_o$ from one guard cell. A two-step protocol was employed (Fig. 3*A–C*, *left*), using different conditioning voltages (dashed lines in Fig. 3*A*, *top left*) used to achieve varying degrees of steady-state activation of $I_{K,out}$. Instantaneous currents recorded on stepping to test voltages between −100 and +50 mV (Fig. 3*A–C*, *arrows left*) are shown in the *I-V* plots (Fig. 3*A–C*, *right*) with the conditioning voltage indicated (*right*). Background currents, determined as the instantaneous current following clamp steps from

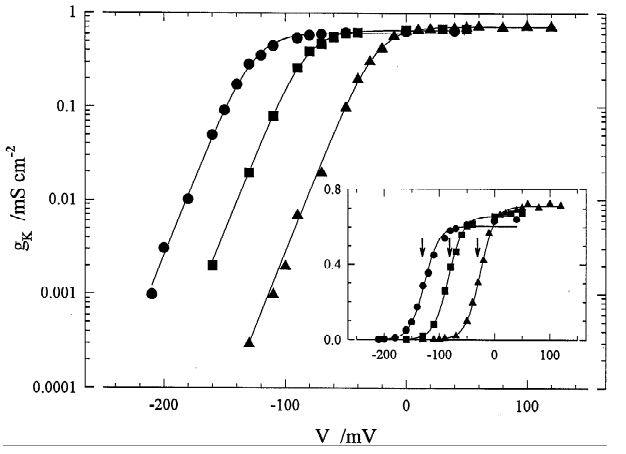

Fig. 4. Ensemble steady-state K^+ channel conductance varies with $[K^+]_o$ and membrane voltage. Conductances from Fig. 3 at 0.1 (●), 1 (■) and 10 mM KCl (▲), and additional data from the same guard cell plotted on a logarithmic ordinate scale as a function of the conditioning voltage step. *Inset:* Data replotted on a linear ordinate scale. Curves were fitted jointly by least-squares minimisation to a Boltzmann function (Eq. 11) with a common gating charge, δ, and yielded a value of 1.87 with values for $V_{1/2}$ (*arrows*) of −129 (●), −81 (■) and −26 mV (▲).

−250 mV have been subtracted in each case. The instantaneous *I-V* curves obtained in this manner demonstrate that, to a first approximation, γ_K was independent of (instantaneous) clamp voltage and show that the conductance, g_K, increased with the conditioning voltage. Only in external $[K^+]_o$ below 1 mM was some nonlinearity evident in the instantaneous *I-V* curves (Fig. 3*A*, *top right*), consistent with constant field expectations for large substrate gradients. Since, in practice, a constant field approach [*see* Hodgkin & Katz, 1949, *not shown*] and the Eq. 10 gave similar results in determining steady-state conductance-voltage ($g_{K,out}$-*V*) relations, the more convenient linear approach has been used for routine calculations.

Figure 4 summarizes the results of a number of instantaneous $g_{K,out}$-*V* measurements, including those in Fig. 3, from the same guard cell. Comparable results were obtained in the other 12 cells subjected to the analysis and are included in Table 1. As shown, the conductances have been fitted jointly to a Boltzmann function (Eq. 4 provides a more detailed approach; *see* Accommodating $[K^+]_o$-dependence of $I_{K,out}$ in Serial *n*-State Gating Models, below) to quantify the dependencies on conditioning voltage and $[K^+]_o$, such that

$$g = \frac{g_{max}}{1 + e^{\delta F (V - V_{1/2})/RT}} \qquad [11]$$

Here, δ is the (minimum) charge moved within the membrane electric field during channel activation and reflects

Table 1. Sensitivity of the voltage gate for the K^+ outward-rectifier to extracellular K^+ concentration

Parameter	$[K^+]_o$/mM				
	0.1	1	3	10	30
δ	1.88 ± 0.03	1.94 ± 0.05	1.95 ± 0.03	1.87 ± 0.02	1.92 ± 0.06
$V_{1/2}$/mV	−131 ± 6	−84 ± 3	−60 ± 3	−26 ± 2	−4 ± 3
(*n*)	8	10	7	12	7

Steady-state conductance for $I_{K,out}$ from 13 *Vicia* guard cells determined from instantaneous $I_{K,out}$-V relations (*see* Figs. 2 and 3). Data sets were fitted to the Boltzmann function (Eq. 11) to obtain the apparent gating charge, δ, and the voltage for half-maximal conductance, $V_{1/2}$. Values are means ± SE of (*n*) data sets at each K^+ concentration.

the ''gain'' inherent to the voltage sensitivity of gating, while $V_{1/2}$ is the voltage at which $g = 0.5\ g_{max}$ and provides a reference for the $[K^+]_o$ sensitivity of gating. For the data shown in Fig. 4, the analysis yielded a δ of 1.87 and $V_{1/2}$ was displaced positive-going with increasing $[K^+]_o$ concentrations giving values for $V_{1/2}$ of −129, −81 and −26 mV at 0.1, 1.0 and 10 mM $[K^+]_o$, respectively (*inset, arrows*). Pooled results from all 13 cells gave a mean shift in $V_{1/2}$ of +52 ± 2 mV/$[K^+]$ decade and δ of 1.91 ± 0.04 (range, 1.82–2.03, consistent with an e-fold rise in current per (+)12.8 mV. The mean $g_{K,max}$ in 10 mM $[K^+]_o$ was 0.68 ± 0.07 mS cm^{-2}.

Extracellular K^+ Affects the Voltage-dependence of $I_{K,out}$ Activation and Deactivation

Extracellular K^+ was reported previously to slow the activation kinetics for $I_{K,out}$ at any one voltage (Blatt, 1988*b*). We found that K^+ outside also accelerated $I_{K,out}$ deactivation upon negative steps to voltages below −75 mV. Figure 5 summarizes the relaxation kinetics determined for $I_{K,out}$ as a function of clamp voltage after conditioning voltage steps to −250 mV (activation) or +50 mV (deactivation) for all 13 cells subjected to analysis. Activation halftimes were taken directly from current traces (Blatt, 1988*b*). Deactivation kinetics for $I_{K,out}$ were well-described by sums of two exponentials, especially for measurements in 0.1 and 1.0 mM $[K^+]_o$ (*see* Fig. 5*A*). Both fast- and slow-decaying components showed appreciable sensitivity to membrane voltage, but only the latter was affected by $[K^+]_o$ (Fig. 5*B*). In this case, increasing $[K^+]_o$ decreased the halftime for current decay at any one voltage — at −150 mV from approximately 140 msec in 0.1 mM $[K^+]_o$ to 65 msec in 10 mM $[K^+]_o$ — the graphical result being a shift of the apparent voltage dependence for deactivation to the right along the voltage axis. Together, the relaxation times for any one $[K^+]_o$ suggest a maximum function of voltage with values declining at more positive voltages corresponding

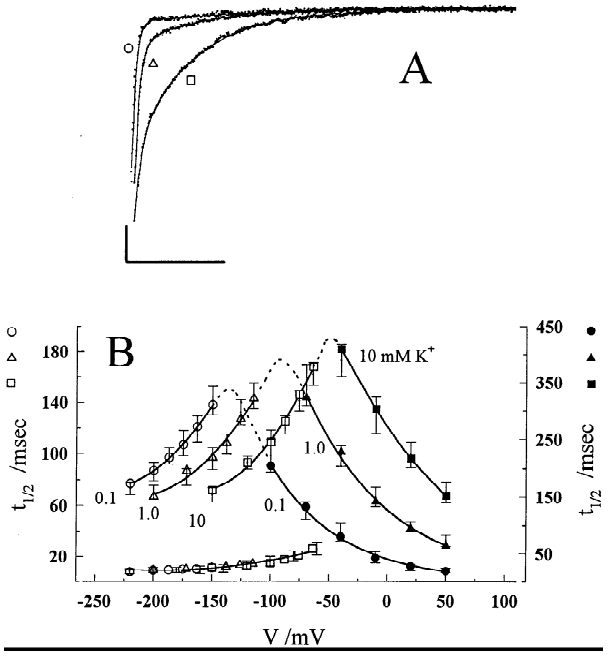

Fig. 5. Extracellular K^+ shifts the voltage-dependence of activation and deactivation halftimes for $I_{K,out}$ in parallel. (*A*) Ensemble K^+ channel ''tail'' currents recorded from one *Vicia* guard cell bathed in 5 mM Ca^{2+}-HEPES, pH 7.4, with 0.1 (○), 1 (△) and 10 mM KCl (□). Currents were recorded at −200 (○), −150 (△) and −100 mV (□) following 2-sec conditioning steps to +20 mV. Background currents have been subtracted (*see* Fig. 2) and data points omitted at times <4 msec to avoid capacitative transients. Solid curves are least-squares fittings to the sum of two exponentials (*see* below). Scale: horizontal, 200 msec; vertical, 10 μA cm^{-2}. (*B*) Summary of halftimes for $I_{K,out}$ activation and deactivation from 13 guard cells. Symbols (activation, filled; deactivation, open) are results of analyses for the cell in Fig. 3. Activation halftimes taken directly from current traces as time to the half-maximum value of the time-dependent current. Deactivation halftimes determined from time constants obtained by fitting current traces to sums of two exponentials (*see* (*A*)). Solid lines are empirical fits to 2nd order polynomials, but show the parallel and roughly a 55-mV shift in activation and deactivation (slow component only) characteristics with each $[K^+]_o$ decade. Dotted lines indicate the anticipated maximum function characteristics for $t_{1/2}$ (*see* text).

to the activation kinetics and at more negative voltages to deactivation kinetics. Furthermore, increasing $[K^+]_o$ shifted this apparent bell-shaped curve to the right along the voltage axis in parallel with the $g_{K,out}$-V curves (*see* Fig. 3).

Ion-dependent Gating is Specific for Extracellular Alkali Cations

Although the results above suggested a role for $[K^+]_o$ in modulating $I_{K,out}$ gating, they offered fewer clues about the physical nature of the interaction between extracellular K^+ and the K^+ channels. The absence of an effect on δ (*see* Fig. 3) argued against a direct action on the voltage sensor itself. However, the $[K^+]_o$ sensitivity of the $g_{K,out}$-V curve might be understood either as a specific effect of extracellular K^+ on the channels or as a consequence of a general charge screening and distortion of the voltage sensed by the channels in the membrane.

To distinguish between these two possibilities, measurements were carried out after substituting $[K^+]_o$ with the alkali cations Cs^+, Rb^+ and Na^+ to examine the specificity of action on $g_{K,out}$ and its voltage-dependence. Figure 6 shows current traces and a synopsis of $I_{K,out}$ activation and deactivation halftimes from one guard cell exposed to 10 mM alkali cation concentrations. Quantitatively similar results were obtained in 7 independent experiments (*see* Table 2). Both Rb^+ and, to a lesser extent, Cs^+ were effective substitutes for extracellular K^+ and displaced the characteristics for activation and for the slow-decaying component of $I_{K,out}$ deactivation along the voltage axis. Substitution with 10 mM Na^+, however, was followed by membrane hyperpolarization to a voltage equivalent to that recorded in 0.1 mM $[K^+]_o$ (Fig. 1, *inset*), and yielded equivalent current relaxation kinetics (compare Fig. 6*A*, *C* and Fig. 2; currents recorded on negative-going voltage steps in Na^+ were small and precluded further analysis of the current deactivation).

A similar relationship was found in the steady-state current and conductance characteristics. Both 10 mM Rb^+ and Cs^+ displaced the I-V and $G_{K,out}$-V curves positive-going with Rb^+ roughly equivalent in effect to K^+ and Cs^+ only marginally less effective, while the voltage-dependent characteristics in 10 mM Na^+ were comparable with those recorded in 0.1 mM K^+ (compare Figs. 2 and 4 with Fig. 7). The current was generally, albeit marginally reduced when K^+ was substituted with Rb^+ and Cs^+ (Fig. 7*A*), declining by 84 ± 6% at 0 mV ($n = 7$). However, the voltage-dependence of the relative conductance ($g_K/g_{K,max}$) in every case yielded common values for δ between curves from any one guard cell (Fig. 7*B*). Table 2 summarizes these results along with bi-ionic equilibria obtained from tail current analyses (Blatt, 1992) and shows a parallel between the efficacy of the alkali cations in shifting the $g_{K,out}$-V relation and their relative selectivities for the channel pore.

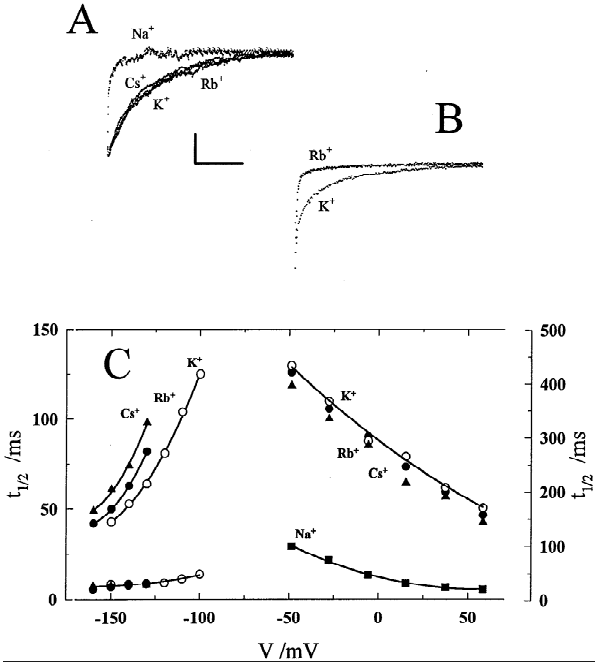

Fig. 6. The monovalent cations Cs^+ and Rb^+, but not Na^+, substitute for external K^+ in modifying the voltage-dependence for K^+ channel activation and deactivation kinetics. Data from one *Vicia* guard cells bathed in 5 mM Ca^{2+}-HEPES, pH 7.4 with 10 mM KCl and following substitution with CsCl, RbCl and NaCl. Cell parameters: surface area, 5.6×10^{-5} cm^2; volume, 6.8 pl; aperture, 13.5 μm. (*A*) Currents recorded on stepping the voltage from a holding potential of −200 to +30 mV. Current traces have been scaled to a common ordinate (*see* Fig. 7 for current amplitudes). Scale: horizontal, 400 msec. Activation in CsCl and RbCl was virtually superimposable with $I_{K,out}$ kinetics in the same concentration of KCl. (*B*) Tail currents recorded on stepping from a holding potential of +30 to −150 mV in the presence of external K^+ and Rb^+. Initial and final (*not shown*) currents differed by less than 3% in these instances. Current amplitude was much reduced in Cs^+ (*not shown*) consistent with the ability of the cation to permeate the channel. Scale: horizontal, 50 msec; vertical, 10 μA cm^{-2}. (*C*) Halftimes for $I_{K,out}$ activation and deactivation as a function of clamp voltage. Activation halftimes taken directly from current traces. Deactivation halftimes determined from time constants obtained by fitting current traces to sums of two exponentials (*see* Fig. 5). Solid lines are empirical fits to 2nd order polynomials, and show a shift in activation and deactivation (slow component only) comparable to that with 10 mM K^+ (○) in 10 mM Rb^+ (●) and Cs^+ (▲).

Extracellular Ca^{2+} Affects Deactivation but not Activation of $I_{K,out}$

Multivalent cations, especially Ca^{2+}, often effect dramatic shifts in the voltage-dependence of channel gating by virtue of their ability to mask charges at the membrane surface (Hille, 1992; Woodhull, 1973; Hille, Woodhull & Shapiro, 1975). Nonetheless, neither Ca^{2+}

Table 2. Ionic selectivities of the K^+ channel pore and of its gate in *Vicia* stomatal guard cells

Function	Relative selectivity			
	K^+	Rb^+	Cs^+	Na^+
P_x/P_K	1.00	0.58 ± 0.04	0.35 ± 0.03	<0.02
$V^x_{1/2}/V^K_{1/2}$	1.00	0.96 ± 0.07	0.51 ± 0.04	0.010 ± 0.008

Relative selectivity for permeation (P_x/P_K) determined from constant field approximation and the reversal potential of $I_{K,out}$ tail currents under bi-ionic conditions (Blatt, 1992). Selectivity of the gate was determined from the shift in $V_{1/2}$ with each alkali cation relative to K^+ as $V^x_{1/2}/V^K_{1/2} = \exp((V^x_{1/2} - V^K_{1/2})F/RT)$ and parameter values were obtained from Eq. 11 as in Fig. 4. Data are means ± SE of 7 independent experiments.

nor Mg^{2+} mimicked the effect of $[K^+]_o$ on gating. Raising $[Ca^{2+}]_o$ from 0.1 to 10 mM reduced $I_{K,out}$ overall by as much as 2-fold (Fig. 8*A*), but in a voltage-independent manner so that neither the relative steady-state conductance characteristic, $V_{1/2}$ nor δ were altered (Fig. 8*B*). Equally, $[Ca^{2+}]_o$ modified the current kinetics. By contrast to the effect of $[K^+]_o$, however, the divalent accelerated $I_{K,out}$ deactivation at voltages negative of −75 mV without a measurable effect on current activation at more positive voltages (Fig. 9*A*,*B*). Furthermore, analyses of $I_{K,out}$ deactivation showed that raising $[Ca^{2+}]_o$ influenced the halftimes of both fast and slow components (Fig. 9*C*). Equivalent results were obtained in 5 independent experiments and qualitatively similar behaviour was observed in 3 further experiments on adding 10 mM Mg^{2+} to the bath (*not shown*). Thus, juxtaposing the gating characteristics showed distinct actions in each case that militated against simple charge screening as an explanation for the $[K^+]_o$-dependent gating of $I_{K,out}$ (*see* Discussion).

Cooperativity of Membrane Voltage and $[K^+]_o$ in Gating

The data in Figs. 2–5 implicate a close relationship between a ''voltage-dependent gate'' and a ''K^+-dependent gate'': half-maximal activation of $g_{K,out}$ in 10 mM $[K^+]_o$ was achieved at −26 mV in Fig. 4, but the same level of activity was observed in 1 mM $[K^+]_o$ when the voltage was driven an additional 55 mV inside negative. It was as if the affinity of this ''K^+ gate'' for extracellular K^+ were increased by membrane hyperpolarization — in other words, as if gating depended on K^+ binding at a site well within the membrane electric field.

To explore this relationship further, data from all 13 guard cells — including the results in Fig. 4 and those of additional measurements at 3 and 30 mM $[K^+]_o$ — were normalized to the maximum $g_{K,out}$, the complement ($=1 - g_K/g_{K,max}$) calculated, and plotted as a function of $[K^+]_o$

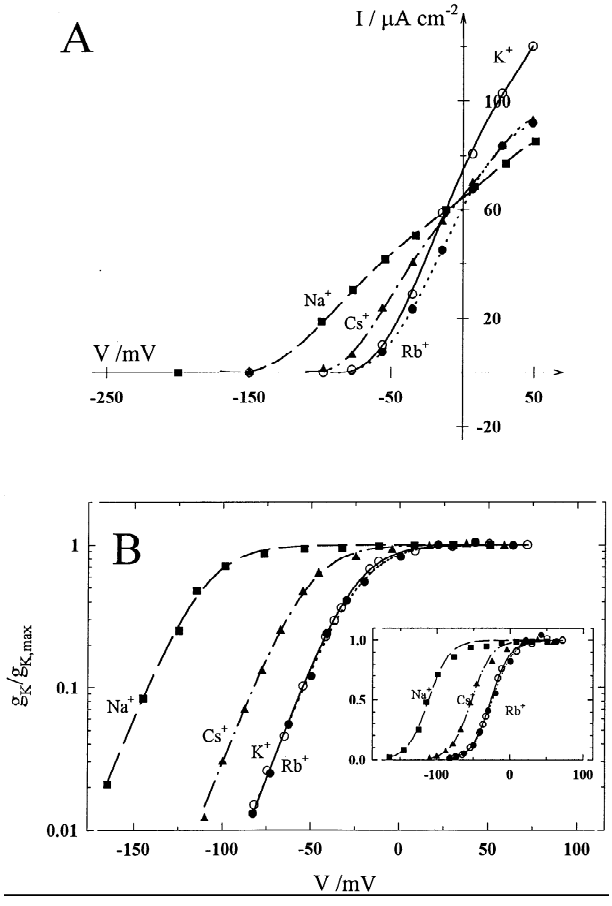

Fig. 7. Rb^+ and Cs^+, but not Na^+, substitute for external K^+ in modifying the steady-state voltage-dependence of K^+ channel conductance g_K. Data from the same *Vicia* guard cell as in Fig. 6. (*A*) Steady-state *I-V* characteristics for the ensemble K^+ channel current determined from positive-going voltage clamp steps as in Fig. 1*C* in the presence of 10 mM K^+ (○) outside and following substitutions with 10 mM Rb^+ (●), Cs^+ (▲), and Na^+ (■). Curves are least-squares fittings to a Boltzmann function (Eq. 11) with δ held in common between data sets (*see below*), and yielded a value of 1.92. Conductance maxima were 8.8 (K^+), 6.1 (Rb^+), 5.5 (Cs^+) and 3.9 mS cm^{-2} (Na^+). Tail current analyses (*not shown*) gave current reversal potentials of −83 mV (K^+), −94 mV (Rb^+), −114 mV (Cs^+) and <−170 mV (Na^+). (*B*) Relative steady-state conductance, $g_K/g_{K,max}$ determined as in Figs. 3 and 4, and plotted on logarithmic scale (and *inset*, on linear scale) as a function of holding potential. Curves are least-squares fitting to a Boltzmann function (Eq. 11) with δ held jointly between data sets. Parameter values were: δ, 1.93; $V_{1/2}$, −111 (Na^+), −53 (Cs^+), −29 (K^+) and −27 (Rb^+).

at each clamp voltage between −120 and +20 mV. The pooled data for selected voltages are included in Fig. 10*A*. The analysis shows that $[K^+]_o$ reduced the relative conductance in a markedly voltage-dependent manner and that an equivalent conductance was realised at lower K^+ concentrations with negative-going membrane voltage. Furthermore, the conductance complement did not follow as a simple hyperbolic (Michaelian) function of $[K^+]_o$, but was sigmoidal, especially at the more positive

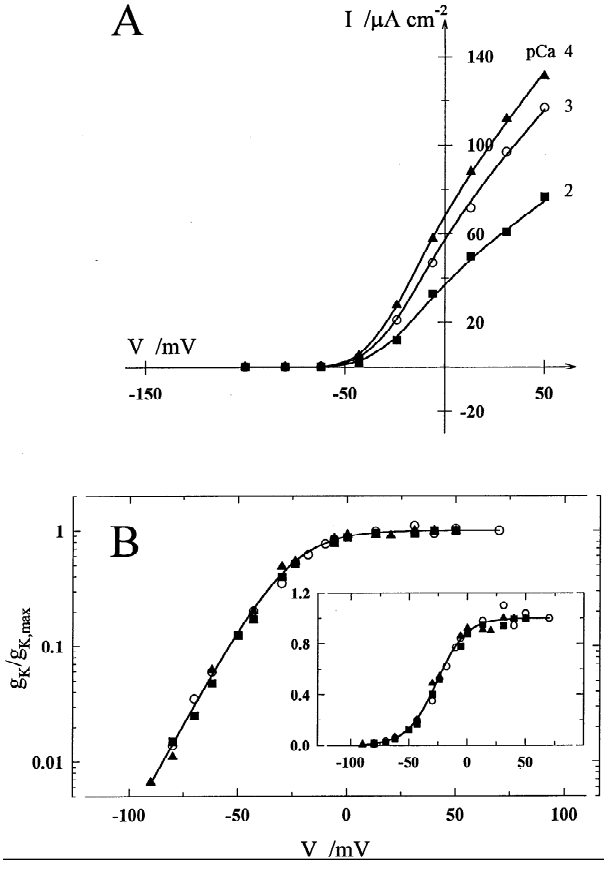

Fig. 8. External Ca^{2+} fails mimic the action of external K^+ in modifying the steady-state voltage-dependence of the relative conductance $g_K/g_{K,max}$. Data from one *Vicia* guard cell bathed in 5 mM K^+-HEPES, pH 7.4, with 7.5 mM KCl (= 10 mM$[K^+]_o$) and 0.1 (▲), 1 (○) and 10 mM $CaCl_2$ (■). (*A*) Steady-state *I-V* characteristics for the ensemble K^+ channel current determined from positive-going voltage clamp steps as in Fig. 2. Curves are least-squares fittings to a Boltzmann function (Eq. 11) with δ held in common between data sets (*see below*), and yielded a value of 1.94. Conductance maxima were 0.85 (▲), 0.72 (○) and 0.41 (■) mS cm^{-2}. (*B*) Relative steady-state conductance, $g_K/g_{K,max}$ determined as in Figs. 3 and 4, and plotted on logarithmic scale (and inset, on linear scale) as a function of holding potential. Curve is from least-squares fitting to a Boltzmann function (Eq. 11). Parameter values were: δ, 1.94; $V_{1/2}$, −25 mV.

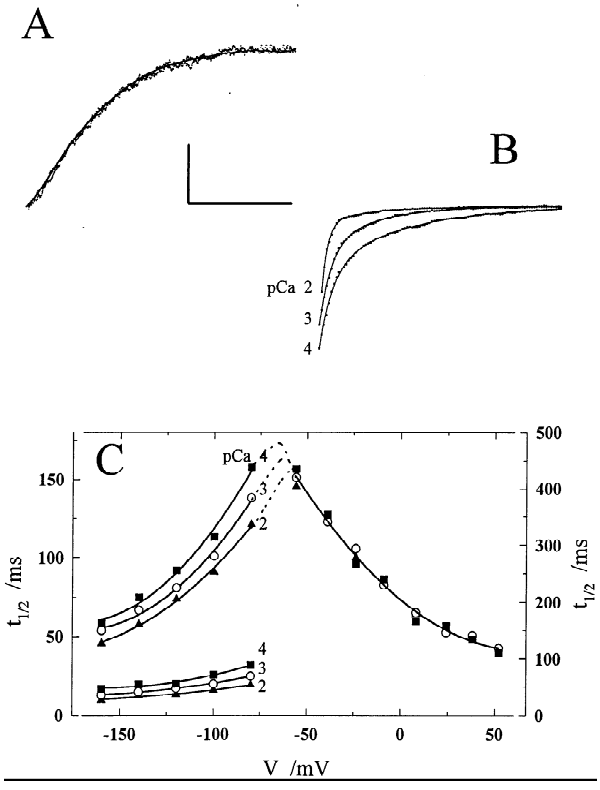

Fig. 9. External Ca^{2+} fails to mimic the effect of $[K^+]_o$ in modifying the voltage-dependence for K^+ channel activation and deactivation kinetics. Data from one *Vicia* guard cell bathed in 5 mM K^+-HEPES, pH 7.4, with 7.5 mM KCl (= 10 mM $[K^+]_o$) and 0.1 (■), 1 (○) and 10 mM $CaCl_2$ (▲). Cell parameters: surface area, 5.2×10^{-5} cm^2; volume, 6.4 pl; aperture, 12.0 μm. (*A*) Currents recorded on stepping the voltage from a holding potential of −200 mV to +30 mV. Current traces have been scaled to a common ordinate. Data points are for 0.1 and 10 mM $CaCl_2$. Current trace in 1 mM $CaCl_2$ indicated by solid curve (5th-order polynomial fitting) for clarity. Scale: horizontal, 500 msec. Activation of $I_{K,out}$ was superimposable at all three $[Ca^{2+}]_o$. (*B*) Tail currents recorded on stepping from a holding potential of +30 to −150 mV, shown fitted by least-squares to sums of two exponentials (below). Scale: horizontal, 50 msec; vertical 50 μA cm^{-2}. (*C*) Halftimes for $I_{K,out}$ activation and deactivation as a function of clamp voltage. Activation halftimes taken directly from current traces were unaffected by $[Ca^{2+}]_o$. Deactivation halftimes from fitting current traces to sums of two exponentials. Solid lines are empirical fits to 2nd order polynomials, and show a shift in both slow and fast exponential components of deactivation kinetics. Dotted lines indicated the anticipated maximum function for $t_{1/2}$ (*see text*).

voltages, consistent with a cooperative action of multiple K^+ ions on the gate. Joint fittings of the data sets at each voltage were carried out to the Hill Equation for cooperative binding (Segel, 1993)

$$g_{K,\mathrm{comp}} = \frac{[K^+]^n}{K_s^n + [K^+]^n} \qquad [12]$$

where $g_{K,comp}$ is the conductance complement, K_s is the apparent dissociation constant, and n is the Hill coefficient for binding of n K^+ ions. Analyses were carried out with n held in common between data sets so that only K_s varied with clamp voltage. Best fittings were obtained with a value of 1.89 ± 0.8 for n. However, the analysis yielded visually and statistically equivalent results when n was fixed at a value of 2 as shown in Fig. 10*A*. A summary of K_s derived from these fittings is shown in Fig. 10*B*. Linear regression of the binding parameter (Fig. 10*B*, *solid line*) indicated an e-fold rise in apparent affinity for K^+ per (−)23.9 mV change in membrane voltage.

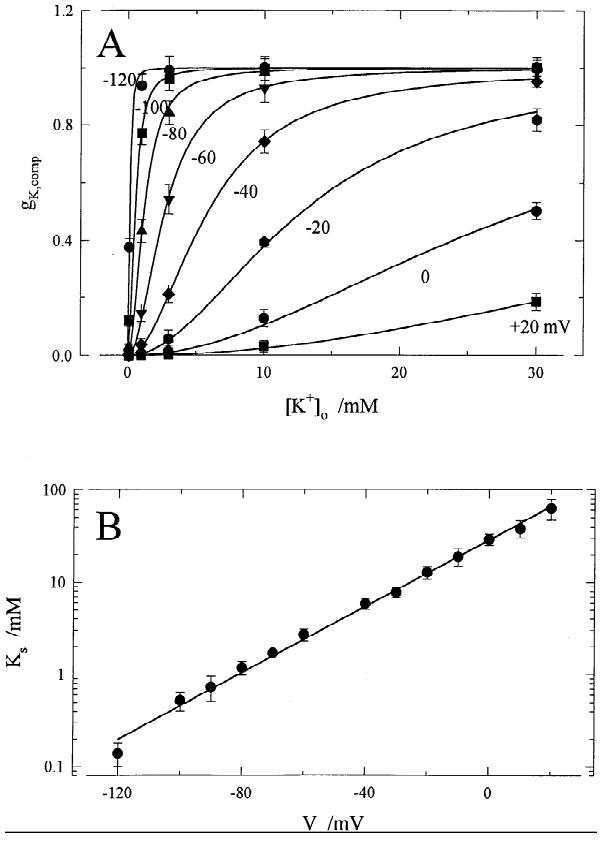

Fig. 10. The K^+-sensitivity of $I_{K,out}$ gating is a cooperative function of extracellular K^+. (*A*) Data from 13 guard cells plotted as the relative conductance complement, $g_{K,comp}$ [$= 1 - (g_K/g_{Kmax})$] against $[K^+]_o$ for voltages between −120 and +20 mV. Curves are the results of least-squares fitting to the Hill Equation (Eq. 12) with *n* held in common between data sets so that only the apparent affinity, K_s, varied with clamp voltage. Best fittings were obtained with a value of 1.89 ± 0.8 for *n*. Statistically equivalent results were obtained (*as shown*) when *n* was fixed at a value of 2. (*B*) Values for K_s from (*A*) as a function of clamp voltage. Linear regression (*solid line*) indicates an e-fold rise in apparent affinity for K^+ per (−)23.9 mV change in membrane voltage.

Accommodating $[K^+]_o$-dependence of $I_{K,out}$ in Serial n-State Gating Models

The current behavior outlined above points to a specific kinetic correspondence between $[K^+]_o$ and membrane voltage with the gating process. Hence, an important question was whether the $[K^+]_o$- and voltage-dependence of the K^+ channels might be accommodated within a stochastic framework for channel gating. Four primary features of $I_{K,out}$ guided our selection of minimum reaction-kinetic models for gating of the current: (i) activation of $I_{K,out}$ was sigmoidal, indicating the presence of at least two exponential components to current relaxations (Figs. 2, 3 and 5); (ii) membrane voltage and $[K^+]_o$ were interactive in determining the current kinetics and $g_{K,out}$ (Figs. 4 and 5); (iii) increasing $[K^+]_o$ slowed current activation; and (iv) $[K^+]_o$ did not influence the apparent gating charge, δ, associated with the voltage-dependence of $g_{K,out}$ (Figs. 4 and 6).

Of these features, the first is consistent with *n*-state models comprising a minimum of two closed states that lead serially to one or more open states of the channel. The fourth point justified a simple kinetic distinction between the voltage and $[K^+]_o$ parameters. Finally, the second and third features discounted gating models in which the final transition from closed to open state of the channel was governed by $[K^+]_o$, or in which $[K^+]_o$- and voltage-dependent transitions from closed states were isolated, connecting only via the open state(s) of the channel.[1] So, in general, a choice among gating models was restricted to serial systems with two or more closed states of the channel (C_2, C_3, . . . C_n) and a terminal open state (O_1)

$$C_n \underset{k_{n(n-1)}}{\overset{k_{(n-1)n}}{\rightleftharpoons}} \ldots \underset{k_{43}}{\overset{k_{34}}{\rightleftharpoons}} C_3 \underset{k_{32}}{\overset{k_{23}}{\rightleftharpoons}} C_2 \underset{k_{21}}{\overset{k_{12}}{\rightleftharpoons}} O_1 \qquad [13]$$

in which one or more of the reaction constants (k_{12}, k_{21}, k_{23}, k_{32}, . . . $k_{(n-1)n}$, $k_{n(n-1)}$) described voltage- and $[K^+]_o$-dependent state transitions with the exception of k_{12} and k_{21} in the final transition ($C_2 \rightleftharpoons O_1$) which were voltage-dependent only. The simplest case that satisfied these requirements comprised three states and four reaction constants (Scheme [1]) in which each of the reaction constants includes a voltage dependent coefficient. Additionally we surmised that the reaction constant k_{23} must subsume a K^+ concentration factor (*see* Materials and Methods) to accommodate K^+ binding outside, because increasing $[K^+]_o$ acted as if to draw channels out of the open state (Figs. 4 and 10).

In fact, for comparative purposes fittings were carried out with K^+ binding assigned to each of the four reaction constants in turn. Data sets from five independent experiments (5 cells) — the data in Figs. 3–5 representing one set — were subjected to analysis using Eqs. 4 and 5. Within each data set, reaction constants and voltage-sensitivity coefficients were sought by joint fitting over a range of voltages and $[K^+]_o$. In each case, best results were obtained with K^+ binding assigned to the pseudo-3-state reaction constant k_{23}, but nonetheless yielded poor approximations for $g_{K,out}$, for current activation in 0.1 mM $[K^+]_o$ and for deactivation in 0.1 and 1

[1] The alternative, that the $[K^+]_o$-sensitive transition feeds directly into the open state, would imply that increasing $[K^+]_o$ must always lead to faster current relaxations (Eq. 4). This was not the case for $I_{K,out}$ activation (Figs. 1 and 2), however, indicating that $[K^+]_o$ must affect one or more state transitions that are removed from the open state.

mM $[K^+]_o$. Similar, albeit statistically somewhat poorer fittings, were obtained when K^+ binding was associated with the pseudo-3-state reaction constant k_{32} and gave an inverse dependence on $[K^+]_o$ ($=k^o_{32}/[K^+]_o$). This apparent paradox with mass action can be understood if channel gating includes a fourth (hidden) state that communicates with state C_3 so that

$$C_4 \underset{k_{43}}{\overset{k_{34}}{\rightleftharpoons}} C_3 \underset{k_{32}}{\overset{k_{23}}{\rightleftharpoons}} C_2 \ \ldots \qquad [14]$$

where, with respect to external $[K^+]_o$, $k_{23} = k_{23}{}^o[K^+]_o$ and $k_{34} = k_{34}{}^o[K^+]_o$. In this case, the pseudo-3-state reaction constants, here denoted with the index ^{3} as k^3_{23} and k^3_{32}, subsume these rate constants (Gradmann, Kleiber & Hansen, 1987) so that

$$k^3_{32} = \frac{k_{43}k_{32}}{k_{34}[K^+]_o + k_{32}} \qquad [15a]$$

and

$$k^3_{23} = \frac{k_{23}[K^+]_o k_{34}[K^+]_o}{k_{34}[K^+]_o + k_{32}} \qquad [15b]$$

Factoring out $[K^+]_o$ thus shows that dependencies of k^3_{32} on $[K^+]_o^{m32}$ with $-1 \leqslant m_{32} \leqslant 0$ and of k^3_{23} on $[K^+]_o^{m23}$ with $1 \leqslant m_{23} \leqslant 2$ are expected. Submitting the data sets to analyses with k^3_{32} and k^3_{23} including the mass action coefficients m_{23} and m_{32} explicitly (*see* Materials and Methods) gave satisfactory results in all five data sets with roughly equivalent voltage- and $[K^+]_o$-sensitivities between the reaction constants. The analysis for the data in Figs. 3–5 is shown in Figs. 11 and 12 and the means of all five analyses are included in Table 3. The analyses yielded values consistent with previous estimates of an apparent gating charge of 2 (Fig. 4) and binding of 2 K^+ in modulating the voltage-sensitivity of $g_{K,\text{out}}$ (Fig. 10).

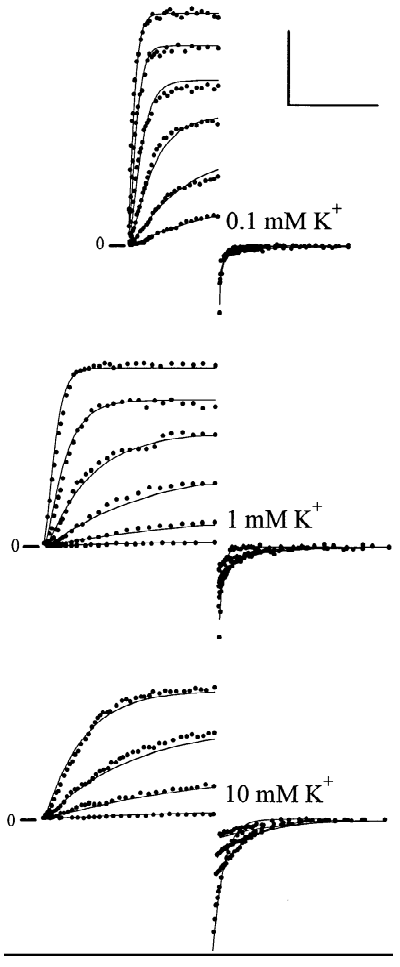

Fig. 11. Dynamic characteristics of the *Vicia* guard cell K^+ current is consistent with a stochastic 4-state (pseudo-3-state) model for channel gating. Current traces for voltage-dependent activation and deactivation from the same cell as in Figs. 3–5 were fitted jointly, together with the steady-state conductances (Fig. 12), by least-squares using Eqs. 4, 5 and 15. Clamp parameters, activation: conditioning voltage, −200 mV; test voltages (6, last 4 only in 10 mM $[K^+]_o$), −100 to +50 mV. Clamp parameters, deactivation: conditioning voltage, +20 mV; test voltages (4), −220 to −180 mV (0.1 mM $[K^+]_o$), −170 to −120 mV (1 mM $[K^+]_o$), −120 to −80 mV (10 mM $[K^+]_o$). Data points in the current traces were selected at standard intervals to reduce the data sets to a manageable size. Scale: horizontal, 400 msec (activation) or 200 msec (deactivation); vertical, 50 μA cm^{-2} (activation) or 25 μA cm^{-2} (deactivation). Solid lines are the results of the analysis. Parameter values are listed in Table 3. See text for further details.

Discussion

The action of extracellular K^+ in gating the K^+ channels of *Vicia* guard cells marks a departure in understanding the control of ion channel activity in plants and sets the K^+ current apart from other outward-rectifiers known in animal cells. Four key lines of evidence support a role for extracellular K^+ as a ligand gating the K^+ channels. (i) Extracellular K^+ had a profound influence on K^+ channel gating (Figs. 2–5) such that at any one voltage $[K^+]_o$ was able to inhibit the current completely and in a manner consistent with the binding of two K^+ ions per channel (Figs. 10–12). (ii) The cation-dependence of gating showed a specificity for K^+ and, to a lesser extent, for other alkali cations (Figs. 6 and 7) consonant with a single class of binding sites with a moderate to weak field strength (Eisenman series IV, (Eisenman & Horn, 1983)). (iii) by contrast, Ca^{2+} and Mg^{2+} did not alter the voltage-dependence, of g_K, nor did they influence the kinetics for activation of $I_{K,\text{out}}$ (Figs. 8 and 9). (iv) Finally, the effect of K^+ on gating was fundamentally distinct from the ability of the cation to permeate the chan-

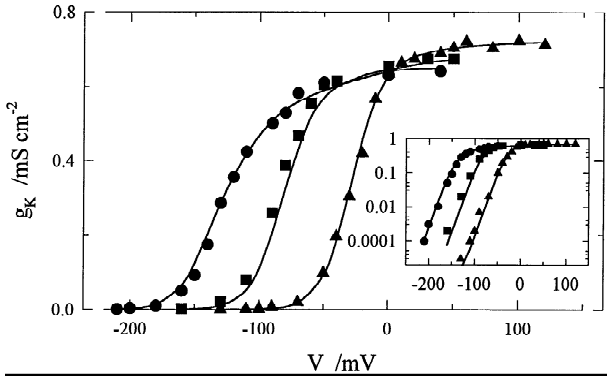

Fig. 12. Steady-state characteristics of the *Vicia* guard cell K^+ current is consistent with a stochastic 4-state (pseudo-3-state) model for channel gating. Steady-state values for $g_{K,out}$ from Fig. 3 were fitted jointly, together with the current traces in Fig. 11, by least-squares using Eqs. 4, 5 and 15. Solid lines are the results of the analysis. Parameter values are listed in Table 3. See text for further details.

nel pore (Figs. 3–5), and quantitatively consistent with a second-order mass action effect of K^+ ions on the channel gate (Figs. 11 and 12).

Separating K^+ Permeation and K^+-dependent Gating

Of these four lines of evidence, the distinction between the roles for K^+ as a permeant, charge-carrying ion and as a gating ligand is fundamental to understanding K^+ channel control in guard cells and higher-plants (Blatt, 1991; Blatt & Thiel, 1993), and may apply to walled eukaryotes generally (Blatt, 1988; Bertl et al., 1993; Bertl & Slayman, 1994; Zhou et al., 1995; Lesage et al., 1996). Gating behavior that depends on extracellular K^+ — so that the *g-V* curve effectively shifts in parallel E_K — is well-documented for a number of K^+ channels in animal cells (Hille & Schwarz, 1978; Hagiwara, Miyazaki & Rosenthal, 1976). Without exception, however, the behaviour in animals has been associated with inward-rectifying K^+ channels and has generally been understood in terms of single-file, multi-site pores in which ions entering from outside the cell displace a blocking molecule or ion entering from the cytoplasmic side (Yang, Jan & Jan, 1995; Hille & Schwarz, 1978). In several tissues, including mammalian heart muscle, this blocking activity is associated with Mg^{2+} and organic ions which are able to enter from the cytoplasmic side, but lodge within the K^+ channels and block passage of K^+ out of the cell (Horie, Irisawa & Noma, 1987; Vandenberg, 1987; Fakler et al., 1994; Yang et al., 1995). In this case, increasing $[K^+]_o$ adds to the electrochemical driving force at any one voltage to relieve channel block by expelling the blocking ion back into the cell. However, such reasoning singularly fails to accommodate K^+-dependent gating in guard cells — as indeed it must for any *outward*-rectifying K^+ channel — simply because gating control and ion permeation draw on two distinct pools of K^+, one inside and the other outside the cell.

Nor are the data consistent with charge screening as a primary mechanism of action for extracellular K^+. In the simplest sense, charge screening affects the electrical field within the membrane by compensating for fixed charges at its surface (Hille et al., 1975; Hille, 1992). The result is to displace the electrical field acting on the channel within the membrane relative to the voltage difference between bulk solutions on either side of the membrane; but in all other respects channel current and gating should remain unchanged. This reasoning does not explain the specificity for alkali cations, and especially K^+, over divalents such as Ca^{2+} that carry a much higher charge density and, hence, would be expected to show a greater efficacy in charge compensation. Indeed, $[Ca^{2+}]_o$ itself was ineffective in displacing the voltage-dependence of $g_{K,out}$ and its action on the $I_{K,out}$ kinetics was biased to current deactivation (Figs. 8 and 9). These characteristics, too, are not easily reconciled with common charge screening models (Armstrong & Cota, 1990; Hille, 1992).

Ligand-dependent Gating is Cooperative and Sensitive to Membrane Voltage

How does extracellular K^+ modulate $g_{K,out}$? Activation of the current was found to be a cooperative function of $[K^+]_o$, consistent with a Hill coefficient of 2, and obeying laws of mass action. These characteristics are broadly consistent with K^+ action as a ligand in gating channel activity and with K^+-binding affinities in the sub- to low-millimolar range. Control of $g_{K,out}$ by K^+ also showed a strong interaction with membrane voltage. Increasing the electrical driving force by (−)23.9 mV to draw K^+ from outside into the membrane suppressed $g_{K,out}$ as much as an e-fold rise in $[K^+]_o$, and the apparent dissociation constant for K^+ rose from approx. 0.5 mM at −100 mV to about 20 mM at 0 mV. So, the simplest interpretation is that two K^+ ions bind at sites on, or associated with, each K^+ channel in order to inactivate it, and that these sites are accessible to the external face of the membrane but deep within the membrane electrical field.

Three possible physical interpretations for K^+ binding and control of $I_{K,out}$ are shown in Fig. 13. In the first case (Pore Model), K^+ or ''K^+-like'' ions are proposed to enter the pore from outside and to bind at a site within the permeation pathway in order to effect block or close the ''K^+ gate''. Increasing concentrations of these ions outside necessitate a corresponding increase in opposing electrical field strength to displace the blocking ion and open the channel. This hypothesis is formally equivalent

Table 3. Voltage- and $[K^+]_o$-dependent kinetic characteristics of the K^+ channel gate in *Vicia* stomatal guard cells

3-State parameter	Values	4-State parameter	Values	at 0 mV, 10 mM $[K^+]_o$
		k^o_{43}/sec^{-1}	38 ± 2	38 ± 2
		k^o_{34}/sec^{-1} M^{-1}	1800 ± 140	18 ± 1
k^o_{32}/sec^{-1}M^{m32}	0.056 ± 0.005	k^o_{32}/sec^{-1}	0.57 ± 0.09	0.57 ± 0.09
k^o_{23}/sec^{-1}M^{m23}	871 ± 19	k^o_{23}/sec^{-1}M^{-1}	159 ± 17	1.6 ± 0.2
k^o_{21}/sec^{-1}	42 ± 3	k^o_{21}/sec^{-1}	42 ± 3	42 ± 3
k^o_{12}/sec^{-1}	3.0 ± 0.3	k^o_{12}/sec^{-1}	3.0 ± 0.3	3.0 ± 0.3
Coefficients of Voltage-dependence:				
		δ_{43}	0.74 ± 0.05	
		δ_{34}	$^-0$[a]	
δ_{32}	0.74 ± 0.06	δ_{32}	$^-0$[a]	
δ_{23}	−0.98 ± 0.03	δ_{23}	−0.98 ± 0.04	
δ_{21}	0.045 ± 0.009	δ_{21}	0.045 ± 0.009	
δ_{12}	−0.42 ± 0.01	δ_{12}	−0.42 ± 0.01	
3-state exponents:				
m_{32}	−0.69 ± 0.09			
m_{23}	1.36 ± 0.08			

[a] Values were consistently smaller than 1×10^{-8} but, otherwise, varied by as much as three orders of magnitude between analyses.

to ''gating particle'' models (Hille, 1992; Frankenhaeuser & Hodgkin, 1957) in which the charge displacement of K^+ or a ''K^+-like'' ion to the binding site(s) confers voltage dependence to the process. A variant of this model, the Trapped-particle Model, proposes an unique (''non-K^+'') charged blocking particle that enters the pore (shown as a doubly-charged particle), becoming trapped from behind by K^+ from outside (Lesage et al., 1996; Ketchum et al., 1995). The alternative interpretation (Allosteric Model) postulates external cation binding/regulatory sites within the membrane electric field that interact with the ''K^+ gate'' of the channel, but are situated outside the permeation pathway.

An attractive feature of the Pore Model lies in the close correspondence between the apparent gating charge for $I_{K,out}$ of 2 (Fig. 2), the apparent cooperativity of 2 K^+ ions in gating (Fig. 10), and the voltage sensitivity for K^+ binding (Fig. 10). The affinity for K^+ showed an e-fold rise per (−)23.9 mV which, with 2 K^+ ions binding, would account fully for the voltage-sensitivity of $g_{K,out}$. This argument aside, we favour the Allosteric Model because, unlike the Pore Model and variants, it identifies external cation access for gating and for permeation unambiguously. A major difficulty with the Pore Model itself lies in separating the actions of K^+ (or another cation) entering from outside and from the inside without violating physical laws or microscopic reversibility. For gating of $I_{K,out}$, it suggests that access of 2 K^+ ions from outside to sites in the pore effects a block of the channel, yet access of K^+ from the inside to the same sites contributes to ion permeation! By contrast, the Allosteric Model separates $[K^+]_o$-sensitivity and K^+ permeation, and can accommodate two sites for parallel binding of K^+. The effect of external K^+ binding in this case might be to alter charge/dipole moments of the gating mechanism or their environment through protein conformational changes (Neyton & Pelleschi, 1991; Armstrong & Lopez-Barneo, 1987). The Trapped-particle Model cannot be wholly excluded at present. However, the added charge on such a particle would not accord so readily with the apparent gating charge of 2 (Fig. 4) associated with the voltage-driven binding of 2 K^+ ions (Fig. 10). Trapping of external Ca^{2+} (Ketchum et al., 1995) seems less likely for the same reason, quite apart from the weak and qualitatively different action of divalents on the current (Figs. 8 and 9).

In formal kinetic terms, these observations are accommodated within the framework of a serial 4-state model comprising a single, terminal state that defines the open conformation of the channel. In the broadest sense, these characteristics are compatible with previous serial models for $I_{K,out}$ gating (Schroeder, 1989; Van Duijn, 1993; Fairley-Grenot & Assmann, 1993; Ilan et al., 1994). However, these earlier attempts did not address the action of extracellular K^+ on gating. Our analysis demonstrates the utility of a reaction-kinetic approach to encompass the action of K^+ consistent with its roles both as a permeant ion and as a ligand for channel gating. Joint analyses with a reduced (pseudo-) 3-state model yielded statistically best, and visually satisfactory approximations to both dynamic current and steady-state conductance characteristics. These results yielded a $[K^+]_o$ sensitivity that was distributed between the 3-state parameters k_{23} and k_{32}, indicating a fourth ''hidden'' state and $[K^+]_o$-dependent transition (Fig. 10 and Table 3). It is worth noting in this context that, in general, the last closed state — C_3 in our 3-state model — does not reflect a fixed end of the chain of possible closed states.

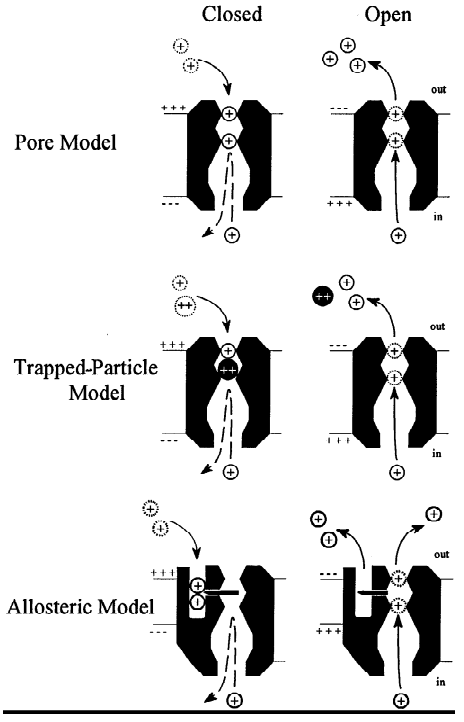

Fig. 13. Physical models for K^+ channel gating. All three models comprise binding sites within the pore that are accessible to K^+ ions from both sides of the membrane. Origins and movement of blocking or gating particles are shown by the dotted particle symbols. Single charged species indicate the nominally permeant ionic species. The Pore Model identifies access from outside with block or closure of the pore and access from inside with ion permeation. The Trapped-particle Model postulates that entry of a nonpermeant blocking particle — as shown from free solution and carrying a double charge, or as particle tethered to the channel outside — results in block or closure when the particle becomes trapped within the pore by a permeant ion entering from behind. The Allosteric Model proposes a set of binding sites, within the membrane electric field but distinct from the pore, that work a gate when both sites are occupied.

Rather, it indicates an open end of which the hallmark is the appearance of non-integer or even negative mass-action binding coefficients (*see* Table 3 and Eq. 15).

Key features of the model are: (i) the presence of two distinct $[K^+]_o$-sensitive reactions (k_{23} and k_{34}) with K^+-binding favoring closed conformations of the channel; (ii) pronounced cooperativity between membrane voltage and $[K^+]_o$ embodied in these reaction constants, but distinct from any action of $[K^+]_o$ on the overall degree of voltage-sensitivity ($=\Sigma\delta_{ij}$, $i,j = 1,2, \ldots 4$); and (iii) kinetic isolation of the $[K^+]_o$-sensitive transitions from the open conformation (O_1) of the channel. Two predictions may be drawn immediately from these characteristics. First, because k_{12} is $[K^+]_o$-insensitive and subsumes a significant fraction of the overall voltage sensitivity within δ_{12}, the mean open lifetimes of the channel ($=1/k_{12}$) should exhibit a significant voltage-dependence, increasing with positive-going voltages, but should be independent of $[K^+]_o$. Conversely, the relative magnitude of δ_{21} anticipates a mean closed lifetime of the channel which is comparatively voltage-insensitive. Third, because the $[K^+]_o$-sensitive steps are isolated from the open state and relatively slow at physiological $[K^+]_o$, the model anticipates bursts of channel activity with burst frequency increasing with membrane voltage and inversely related to $[K^+]_o$ ($C_3 \leftrightharpoons C_2$ transitions). In fact, some of these characteristics have already been identified in outward-rectifying K^+ channels of *Vicia* guard cells. Hosoi, et al. (1988) reported bursts of channel activity with longer periods of inactivity evident as the clamp voltage was driven negative of 0 mV in symmetric 50 mM $[K^+]_o$. They also observed that open times, but not closed times showed a significant voltage dependence between −40 and +100 mV.

It is worth noting that the specificity of gating among the alkali cations paralleled that for cation selectivity within the channel pore itself. Both selectivities consistent with Eisenman series IV predicting binding sites with low to moderate field strength (Eisenman & Horn, 1983). While the characteristics of channel permeation and gating indicate that the two processes are independent, their similar selectivities argues for K^+-dependent gating mediated through binding at energetically comparable site(s) and with little requirement for stripping of the ionic hydration shell. We note that a new class of K^+ channels appear to comprise two ''pore-like'' domains (Salkoff & Jegla, 1995; Ketchum et al., 1995; Zhou et al., 1995) and, at least one of this family found in yeast, exhibits voltage- and K^+-dependent gating characteristics comparable to $I_{K,out}$ (Zhou et al., 1995; Bertl & Slayman, 1994; Vergani et al., 1997). A similar channel structure may account for $I_{K,out}$ in guard cells and other higher-plant cell types (Blatt, 1988*a;* Terry, Tyerman & Findlay, 1991*a*), and suggests one intriguing feature: that these domains function independently in forming the transmembrane pore and access to K^+-binding sites for gating.

Physiological Implications of $[K^+]_o$ Sensitivity

Potassium efflux from the guard cells is mediated predominantly by $g_{K,out}$. The activity of these K^+ channels, together with current through anion channels, provides for net solute (KCl) loss from the cells (Gradmann et al., 1993) and, thus, both currents must act in concert for stomata to close (Blatt & Thiel, 1993). Incredibly, stomatal closure is realised over external KCl concentrations ranging from 0.1 to 100 mM (Willmer & Fricker, 1996) — that is, even as E_K varies over nearly 180 mV within the normal physiological voltage range — and the observation implies a remarkable ability for channel gating to accommodate changes in electrochemical driving force. Here a comparison with the Na^+ channel of the

squid axon is valuable (Hodgkin & Katz, 1949). Gating of this channel is fixed to a narrow voltage range near −40 mV and reducing the external Na^+ concentration — even to 10% of normal seawater so that E_{Na} approaches this voltage — renders the axon inactive to further excitation. In fact, the voltage-dependence of anion channel gating in *Vicia* guard cells has been found to be relatively insensitive to extracellular K^+ and Cl^- (Hedrich & Marten, 1993; Schmidt & Schroeder, 1994). If gating of *both* $I_{K,out}$ and the anion channels in guard cells were confined to a narrow voltage range, at higher $[K^+]_o$ situations could arise favouring net KCl uptake and preventing stomatal closure. So the fact that the voltage sensitivity of $g_{K,out}$ shifts in parallel E_K, with respect to $[K^+]_o$, ensures that K^+ movement through $I_{K,out}$ is directed outward and net solute efflux is favoured regardless of external solute conditions. In short, regulation of the effective voltage-dependence for K^+ and Cl^- efflux can be understood primarily as a consequence of $g_{K,out}$ gating and its $[K^+]_o$-dependence.

This work was possible with the aid of grants from the Gatsby Charitable Foundation, the Royal Society, the Biotechnology and Biological Sciences Research Council, and the University of London Central Research Fund. Travel (M.R.B.) was supported in part by the British Council. D.G. was funded by grants from the Volkswagen Stiftung (I/7127) and from the British Council (313-ARC-X-96/43).

References

Armstrong, C.M., Cota, G. 1990. Modification of sodium channel gating by lanthanum. *J. Gen. Physiol.* **96:**1129–1140

Assmann, S.M. 1993. Signal transduction in guard cells. *Annu. Rev. Cell Biol.* **9:**345–375

Armstrong, F., Leung, J., Grabov, A., Brearley, J., Giraudat, J., Blatt, M.R. 1995. Sensitivity to abscisic acid of guard cell K^+ channels is suppressed by *abi1-1*, a mutant *Arabidopsis* gene encoding a putative protein phosphatase. *Proc. Natl. Acad. Sci. USA* **92:**9520–9524

Armstrong, C.M., Lopez-Barneo, J. 1987. External calcium ions are required for potassium channel gating in squid neurons. *Science* **236:**712–714

Bertl, A., Klieber, H.G., Gradmann, D. 1988. Slow kinetics of a potassium channel in acetabularia. *J. Membrane Biol.* **102:**141–152

Bertl, A., Slayman, C.L. 1994. Chemical and electrochemical control by K^+ itself, in gating the major outward-rectifier K^+ channel (ypk1) of *Saccharomyces. Biophysical J.* **66:**427

Bertl, A., Slayman, C.L., Gradmann, D. 1993. Gating and conductance in an outward-rectifying K^+ channel from the plasma membrane of *Saccharomyces cerevisiae. J. Membrane Biol.* **132:**183–199

Blatt, M.R. 1987*a*. Electrical characteristics of stomatal guard cells: the ionic basis of the membrane potential and the consequence of potassium chloride leakage from microelectrodes. *Planta* **170:**272–287

Blatt, M.R. 1987*b*. Electrical characteristics of stomatal guard cells: the contribution of ATP-dependent, ''electrogenic'' transport revealed by current-voltage and difference-current-voltage analysis. *J. Membrane Biol.* **98:**257–274

Blatt, M.R. 1988*a*. Potassium channel gating in guard cells depends on external K^+ concentration. *Plant Physiol.* **86:**826*A*(*Abst.*)

Blatt, M.R. 1988*b*. Potassium-dependent bipolar gating of potassium channels in guard cells. *J. Membrane Biol.* **102:**235–246

Blatt, M.R. 1990. Potassium channel currents in intact stomatal guard cells: rapid enhancement by abscisic acid. *Planta* **180:**445–455

Blatt, M.R. 1991. Ion channel gating in plants: physiological implications and integration for stomatal function. *J. Membrane Biol.* **124:**95–112

Blatt, M.R. 1992. K^+ channels of stomatal guard cells: characteristics of the inward rectifier and its control by pH. *J. Gen. Physiol.* **99:**615–644

Blatt, M.R., Armstrong, F. 1993. K^+ channels of stomatal guard cells: abscisic acid-evoked control of the outward rectifier mediated by cytoplasmic pH. *Planta* **191:**330–341

Blatt, M.R., Thiel, G. 1993. Hormonal control of ion channel gating. *Annu. Rev. Plant Physiol. Mol. Biol.* **44:**543–567

Eisenman, G., Horn, R. 1983. Ionic selectivity revisited: the role of kinetic and equilibrium processes in ion permeation through channels. *J. Membrane Biol.* **76:**197–225

Fairley-Grenot, K.A., Assmann, S.M. 1993. Comparison of K^+ channel activation and deactivation in guard cells from a dicotyledon (*Vicia faba* L.) and a graminaceous monocotyledon (*Zea mays*). *Planta* **189:**410–419

Fakler, B., Brandle, U., Bond, C., Glowatzki, E., Konig, C., Adelman, J.P., Zenner, H.P., Ruppersberg, J.P. 1994. A structural determinant of differential sensitivity of cloned inward rectifier K^+ channels to intracellular spermine. *FEBS Lett.* **356:**199–203

Frankenhaeuser, B., Hodgkin, L. 1957. The action of calcium on the electrical properties of squid axons. *J. Physiol.* **137:**218–244

Giraudat, J. 1995. Abscisic acid signalling. *Curr. Biol.* **7:**232–238

Gradmann, D., Blatt, M.R., Thiel, G. 1993. Electrocoupling of ion transporters in plants. *J. Membrane Biol.* **136:**327–332

Gradmann, D., Kleiber, H.-G., Hansen, U.-P. 1987. Reaction kinetic parameters for ion transport from steady-state current-voltage curves. *Biophys. J.* **51:**569–585

Hagiwara, S., Miyazaki, S., Rosenthal, N.P. 1976. Potassium current and the effect of cesium on this current during anomalous rectification of the egg cell membrane of a starfish. *J. Gen. Physiol.* **67:**621–638

Hedrich, R., Marten, I. 1993. Malate-induced feedback regulation of plasma membrane anion channels could provide a CO_2 sensor to guard cells. *EMBO J.* **12:**897–901

Hetherington, A.M., Quatrano, R.S. 1991. Mechanisms of action of abscisic acid at the cellular level. *New Phytol.* **119:**9–32

Hille, B. 1992. *Ionic Channels of Excitable Membranes.* pp. 1–607. Sinauer Press, Sunderland, MA

Hille, B., Schwarz, W. 1978. Potassium channels as multi-ion single-file pores. *J. Gen. Physiol.* **72:**409–442

Hille, B., Woodhull, A.M., Shapiro, B.I. 1975. Negative surface charge near sodium channels of nerve: divalent ions, monovalent ions and pH. *Phil. Trans. Roy. Soc. Lond. B* **270:**301–318

Hodgkin, A.L., Huxley, A.F., Katz, B. 1952. Measurements of current-voltage relations in the membrane of the giant axon of *Loligo. J. Physiol.* **116:**424–448

Hodgkin, A.L., Katz, B. 1949. The effect of sodium ions on the electrical activity of the giant axon of the squid. *J. Physiol.* **108:**37–77

Horie, M., Irisawa, H., Noma, A. 1987. Voltage-dependent magnesium block of adenosine-triphosphate-sensitive potassium channel in guinea pig ventricular cells. *J. Physiol.* **387:**251–272

Hosoi, S., Iino, M., Shimazaki, K. 1988. Outward-rectifying K^+ channels in stomatal guard cell protoplasts. *Plant Cell Physiol.* **29:**907–911

Ilan, N., Schwartz, A., Moran, N. 1994. External pH effects on the depolarization-activated K channels in guard cell protoplasts of *Vicia faba. J. Gen. Physiol.* **104:**807–831

Ketchum, K.A., Joiner, W.J., Sellers, A.J., Kaczmarek, L.K., Goldstein, S.A.N. 1995. A new family of outwardly rectifying potassium

channel proteins with 2 pore domains in tandem. *Nature* **376:**690–695

Lesage, F., Guillemare, E., Fink, M., Duprat, F., Lazdunski, M., Romey, G., Barhanin, J. 1996. A pH-sensitive yeast outward rectifier K^+ channel with 2 pore domains and novel gating properties. *J. Biol. Chem.* **271:**4183–4187

MacRobbie, E.A.C. 1991. Effect of ABA on ion transport and stomatal regulation. *In: Abscisic Acid Physiology and Biochemistry.* pp. 153–168. W.J. Davies and H.G. Jones, editors. Bios Scientific, Oxford

MacRobbie, E.A.C. 1992. Calcium and ABA-induced stomatal closure. *Proc. Roy. Soc. Lond. B. Biol. Sci.* **338:**5–18

Marquardt, D. 1963. An algorithm for fleast-squaires estimation of nonlinear parameters. *J. Soc. Ind. Appl. Math.* **11:**431–441

Neyton, J., Pelleschi, M. 1991. Multi-ion occupancy alters gating in high-conductance, Ca^{2+}-activated K^+ channels. *J. Gen. Physiol.* **97:**641–665

Press, W., Flannerly, B., Teukolsky, S., Vetterling, W. 1986. *Numerical Recipies: The Art of Scientific Computing.* Cambridge University Press, Cambridge

Salkoff, L., Jegla, T. 1995. Surfing the DNA databases for K^+ channels nets yet more diversity. *Neuron* **15:**489–492

Schmidt, C., Schroeder, J.I. 1994. Anion selectivity of slow anion channels in the plasma membrane of guard cells — large nitrate permeability. *Plant Physiol.* **106:**383–391

Schroeder, J.I. 1989. Quantitative analysis of outward rectifying K^+ channel currents in guard cell protoplasts from *Vicia faba. J. Membrane Biol.* **107:**229–235

Schroeder, J.I. 1992. Plasma membrane ion channel regulation during abscisic acid-induced closing of stomata. *Philos. Trans. R. Soc. Lond. B. Biol. Sci.* **338:**83–89

Schroeder, J.I., Raschke, K., Neher, E. 1987. Voltage dependence of K^+ channels in guard-cell protoplasts, *Proc. Natl. Acad. Sci. USA* **84:** 4108–4112

Segel, I.H. 1993. *Enzyme Kinetics.* pp. 1–957. Wiley Interscience, New York

Terry, B.R., Tyerman, S.D., Findlay, G.P. 1991. Ion channels in the plasma membrane of *Amaranthus* protoplasts: one cation and one anion channel dominate the conductance. *J. Membrane Biol.* **121:**223–236

Thiel, G., Blatt, M.R. 1991. The mechanism of ion permeation through K^+ channels of stomatal guard cells voltage-dependent block by Na^+. *J. Plant Physiol.* **138:**326–334

Thiel, G., MacRobbie, E.A.C., Blatt, M.R. 1992. Membrane transport in stomatal guard cells: the importance of voltage control. *J. Membrane Biol.* **126:**1–18

Van Duijn, B. 1993. Hodgkin-Huxley analysis of whole-cell outward rectifying K^+ currents in protoplasts from tobacco cell suspension cultures. *J. Membrane Biol.* **132:**77–85

Vandenberg, C.A. 1987. Inward rectification of a potassium channel in cardiac ventricular cells depends on internal magnesium ions. *Proc. Natl. Acad. Sci. USA* **84:**2560–2564

Vergani, P., Miosga, T., Jarvis, S.M., Blatt, M.R. 1997. Extracellular K^+ and Ba^{2+} mediate voltage-dependent inactivation of the outward-rectifying K^+ channel encoded by the yeast gene *TOK1*. *Febs Lett.*, **405:**337–344

Willmer, C., Fricker, M.D. 1996. *Stomata.* Chapman and Hall. London. 1–375

Woodhull, A.M. 1973. Ionic blockage of sodium channels in nerve. *J. Gen. Physiol.* **61:**687–708

Yang, J., Jan, Y.N., Jan, L.Y. 1995. Control of rectification and permeation by residues in 2 distinct domains in an inward rectifier K^+ channel. *Neuron* **14:**1047–1054

Zhou, X.L., Vaillant, B., Loukin, S.H., Kung, C., Saimi, Y. 1995. Ykc1 encodes the depolarization-activated K^+ channel in the plasma membrane of yeast. *FEBS Lett.* **373:**170–176